Synthesis and Thermoelectric Properties of the New Ternary Bismuth Sulfides $KBi_{6.33}S_{10}$ and $K_2Bi_8S_{13}$

Mercouri G. Kanatzidis,* Timothy J. McCarthy, Troy A. Tanzer,[†]
Li-Heng Chen,[‡] and Lykourgos Iordanidis

*Department of Chemistry and Center for Fundamental Materials Research,
Michigan State University, East Lansing Michigan 48824*

Tim Hogan and Carl R. Kannewurf

*Department of Electrical Engineering and Computer Science,
Northwestern University, Evanston, Illinois 60208*

Ctirad Uher and Baoxing Chen

Department of Physics, University of Michigan, Ann Arbor, Michigan 48109

Received January 9, 1996. Revised Manuscript Received April 24, 1996[⊗]

　　$KBi_{6.33}S_{10}$ and $K_2Bi_8S_{13}$ were synthesized by the direct combination of K_2S/Bi_2S_3 at high temperature (>700 °C). The reaction of $K_2S/3.3Bi_2S_3$ at 800 °C revealed the presence of a new ternary sulfide $KBi_{6.33}S_{10}$ (**I**, 92% yield). The shiny, silver polycrystalline material crystallizes in the orthorhombic space group *Pnma* (No. 62) with $a = 24.05(1)$ Å, $b = 4.100$-(2) Å, $c = 19.44(1)$ Å, $V = 1917(3)$ Å^3, $Z = 4$, and $d_c = 5.828$ g/cm^3. Data with $F_o^2 > 3\sigma(F_o^2)$, 862; no. of variables 108, $2\theta_{max}$ 50°. The final $R/R_w = 4.3/4.7\%$. The structure consists of blocks of Bi_2Te_3- and CdI_2-type units that are connected to form a three-dimensional network with K$^+$ ions located in the channels that run along the *b* axis. The same reaction but with a different reactant ratio at 750 °C gave the new ternary sulfide $K_2Bi_8S_{13}$ (**II**, 94% yield). This compound crystallizes in the monoclinic space group $P2_1/m$ (No. 11) with $a = 16.818(2)$ Å, $b = 4.074(5)$ Å, $c = 17.801(3)$ Å, $\beta = 90.48(1)°$, $V = 1220(2)$ Å^3, $Z = 2$, and $d_c = 5.900$ g/cm^3. Data with $F_o^2 > 3\sigma(F_o^2)$, 1924; no. of variables 131, $2\theta_{max}$ 50°. The final $R/R_w = 7.3/8.2\%$. The structure of the shiny rodlike crystals is closely related to that of **I**. As in I, it also consists of Bi_2Te_3- and CdI_2-type fragments that connect to form K$^+$-filled channels. The two potassium atoms and one bismuth atom are disordered over three sites. Electrical conductivity on **I** show semiconducting behavior with 10^2 S/cm at 300 K. Compound **II** possesses an electrical conductivity of 10^2 S/cm at 300 K. The optical bandgaps of **I** and **II** (0.06–0.24 eV) were estimated by infrared diffuse reflectance measurements. Thermal analysis and thermal conductivity data for **I** and **II** are reported. The thermal conductivity of $KBi_{6.33}S_{10}$ is found to be substantially lower than that of Bi_2Te_3.

Introduction

Group 15 chalcogenide compounds have received considerable attention, due to their potential application as nonlinear optical materials,[1] photoelectrics,[2] and thermoelectrics.[3] The most common application that is unique to group 15 chalcogenides is in the area of thermoelectric cooling materials. The most investigated systems over the past 30 years are various solid solutions of M_2Q_3 (M = As, Sb, Bi; Q = S, Se, Te) compounds.[4] These materials possess high electrical conductivity and thermoelectric power and low thermal conductivity and are excellent materials for thermoelectric applications near room temperature.[5] With these

properties in mind, it is surprising that very little exploratory synthesis of new ternary bismuth chalcogenide phases has been reported. Bi is very attractive for study because of its inert 6s^2 lone pair of electrons which may or may not be manifested structurally in a given compound. Whether the lone pair is stereochemically active or not affects the lattice structure, the electronic structure, and thus the properties of the resulting compounds. Exploration of the solid-state chemistry of Bi is therefore warranted. This issue is related to the larger question of stereochemical activity of a lone pair in compounds with heavy main-group elements in a s^2 configuration.

Outside of the well-known NaCl-type $ABiQ_2$ (A = Li, Na, K; Q = S, Se)[6] compounds, the only other phases that have been fully characterized structurally are $RbBiQ_2$ (Q = S, Se),[7] $CsBi_3S_5$,[8] $RbBi_3S_5$,[9] $Tl_4Bi_2S_5$,[10] α-(β-

(1) (a) Feichtner, J. D.; Roland, G. W. *Appl. Opt.* **1972,** *11*, 993–998 (b) Ballman, A. A.; Byer, R. L.; Eimerl, D.; Feigelson, R. S.; Feldman, B. J.; Goldberg, L. S.; Menyuk, N.; Tang, C. L. *Appl. Opt.* **1987,** *26*, 224–227.
(2) Ibuki, S; Yoschimatsu, S. *J. Phys. Soc. Jpn.* **1955,** *10*, 549–554.
(3) (a) Kaibe, H.; Tanaka,Y.; Sakata, M.; Nishida, I. *J. Phys. Chem. Solids* **1989,** *50*, 945–950. (b) Jeon, H.-W.; Ha, H.-P.; Hyun, D.-B.; Shim, J.-D. *J. Phys. Chem. Solids* **1991,** *4*, 579–585.

(4) (a) Smith, M. J.; Knight, R. J.; Spencer, C. W. *J. Appl. Phys.* **1962,** *33*, 2186–2190. (b) Testardi, L. R.; Bierly, J. N. Jr.; Donahoe, F. J. *J. Phys. Chem. Solids* **1962,** *23*, 1209. (c) Champness, C. H.; Chiang, P. T.; Parekh, P. *Can. J. Phys.* **1965,** *43*, 653–569. (d) Yim, W. M.; Fitzke, E. V. *J. Electrochem. Soc.* **1968,** *115*, 556–560.
(5) (a) Rowe, D. M.; Bhandari, C. M. *Modern Thermoelectrics*; Holt, Rinehart and Winston: London, 1983; p 103. (b) Borkowski, K.; Przyluski, J. *J. Mater. Res. Bull.* **1987,** *22*, 381–387.

)-BaBi$_2$S$_4$,[11] Cs$_3$Bi$_7$Se$_{12}$,[12] Sr$_4$Bi$_6$Se$_{13}$,[13] and BaBiSe$_3$.[14] These compounds have been prepared at high (>450 °C) temperature by direct combination of the elements or alkali carbonates with Bi and S(Se). In addition, mixed Bi/transition metal/Q (Q = S, Se) solid solution systems have been investigated including Cu$_{1+3x}$Bi$_{5-x}$Q$_8$[15] and Mn$_{1-x}$Bi$_{2+y}$Q$_4$.[16] In interesting contrast, bismuth compounds constitute ∼20% of the known naturally occurring sulfo salts, including PbBi$_2$S$_4$ (galenobismuthite),[17] PbCu$_4$Bi$_5$S$_{11}$,[18] CuBi$_5$S$_8$,[19] and PbCuBiS$_3$.[20]

Recently, we have synthesized four new ternary bismuth chalcogenides, β-(γ-)-CsBiS$_2$,[21] K$_2$Bi$_8$Se$_{13}$,[21] and KBi$_3$S$_5$,[22] using A$_2$Q$_x$ (A = K, Cs; Q = S, Se) fluxes at intermediate temperatures below 400 °C that display a wide range of structural diversity. K$_2$Bi$_8$Se$_{13}$ possesses interesting thermoelectric properties with an electrical conductivity of 10^{-2} S/cm and a Seebeck coefficient ranging from −210 to −260 μV/K at room temperature.[21] During our investigation, we noticed that there are several high-temperature A$_2$Q/Bi$_2$Q$_3$ (A = Li, Na, K, Rb, Cs; Q = S, Se, Te) phase diagrams reported in the literature.[23] However, the structural information on the possible phases consists only of unindexed powder X-ray diffraction patterns. It became apparent to us that further work in the synthesis and structural characterization of new A$_x$Bi$_y$Q$_z$ compounds was necessary. This paper describes the high-temperature synthesis, structural characterization, and optical and charge-transport properties of two new compounds, KBi$_{6.33}$S$_{10}$ (**I**) and K$_2$-Bi$_8$S$_{13}$ (**II**). Both of these compounds possess new three-dimensional tunnel frameworks based on Bi$_2$Te$_3$- and CdI$_2$-type fragments with K$^+$ ions found in the channels.

Experimental Section

Reagents. Chemicals in this work were used as obtained: (i) bismuth powder, 99.999+% purity, −100 mesh, Aldrich Chemical Co., Inc., Milwaukee, WI; (ii) sulfur powder, sub-

limed, J. T. Baker Chemical Co., Phillipsburg, NJ; (iii) potassium metal, analytical reagent, Mallinckrodt Inc., Paris, KY; (iv) methanol, anhydrous, Mallinckrodt Inc., Paris, KY; DMF, analytical reagent, diethyl ether, ACS anhydrous, EM Science, Inc., Gibbstown, NJ.

Synthesis. All manipulations were carried out under a dry nitrogen atmosphere in a Vacuum Atmospheres Dri-Lab glovebox. The preparation of K$_2$S is reported elsewhere.[24]

Bismuth Sulfide, Bi$_2$S$_3$. An amount of 2.090 g (10.0 mmol) of Bi and 0.496 g (15.5 mmol) of S were ground thoroughly with a mortar and pestle. The mixture was transferred to a 6 mL Pyrex tube and was subsequently flame-sealed in vacuum (∼10^{-3} Torr). The reaction was heated to 500 °C over 24 h in a computer-controlled furnace, then isothermed at 500 °C for 4 days, followed by cooling to 100 °C at a rate of 4 °C/h, then to 50 °C in 1 h. The product was ground into a fine powder and stored in the glovebox.

KBi$_{6.33}$S$_{10}$ (I). An amount of 0.020 g (0.181 mmol) of K$_2$S and 0.308 g (0.599 mmol) of Bi$_2$S$_3$ were mixed together with a spatula in a glass vial. Several drops of acetone were placed in a quartz tube (9 mm diameter, 6 mL volume), and it was heated with a flame to create a carbon film on the inside surface of the tube. The mixture was transferred to the carbon-coated quartz tube and was subsequently flame-sealed under diffusion pump vacuum (∼10^{-5} Torr). The reaction was heated to 800 °C over a 50 h period in a computer-controlled furnace and then isothermed at 800 °C for 6 days, followed by cooling to 550 °C at a rate of 10 °C/h, then to 50 °C in 10 h. The product was washed with degassed water (50 mL), methanol (20 mL) and ether (20 mL) to remove any trace amounts of K$_2$S. An amount of 0.301 g (92% yield, based on Bi$_2$S$_3$) of shiny silvery polycrystalline material of needle morphology was obtained. Standardless semiquantitative microprobe analysis gave K$_{1.0}$Bi$_{6.1}$S$_{10}$ (average of six acquisitions).

K$_2$Bi$_8$S$_{13}$ (II). The reaction of 0.040 g (0.363 mmol) of K$_2$S and 0.746 g (1.45 mmol) of Bi$_2$S$_3$ was prepared as above using a carbon quoted tube. The mixture was heated to 750 °C over a 40 h period and then isothermed for 6 days, followed by cooling to 550 °C at 10 °C/h, then to 50 °C in 10 h. The product was isolated as above to give 0.739 g (94% yield) of shiny silvery needle crystals and bundles. Microprobe analysis gave K$_{2.0}$Bi$_{8.5}$S$_{13}$ (average of six acquisitions).

The homogeneity of **I** and **II** was confirmed by comparing the observed and calculated X-ray powder diffraction patterns. The d_{hkl} spacings observed for the bulk materials were compared and found to be in good agreement with the d_{hkl} spacings calculated from the single-crystal data.[25] The results are listed in the supporting information.

Physical Measurements

Infrared Spectroscopy. Infrared diffuse reflectance spectra of **I** and **II** were recorded as a solid. The sample was ground into a powder prior to data acquisition. The spectra were recorded in the mid-IR region (4000−400 cm^{-1}, 4 cm^{-1} resolution) with the use of a Nicolet 740 FT-IR spectrometer equipped with a diffuse reflectance attachment.

Electron Microscopy. Quantitative microprobe analysis of the compounds was performed with a JEOL JSM-35C scanning electron microscope (SEM) equipped with a Tracor Northern energy dispersive spectroscopy (EDS) detector. Data were acquired using an accelerating voltage of 20 kV and a 1 min accumulation time.

UV/Vis/Near-IR Spectroscopy. Optical diffuse reflectance measurements were made at room temperature with a Shimadzu UV-3101PC double-beam, double-monochromator spectrophotometer. The instrument was equipped with an integrating sphere and controlled by a personal computer. The measurement of diffuse reflectivity can be used to obtain

(6) (a) Boon, J. W. *Recl. Trav. Chim. Pays-Bas* **1944**, *63*, 32. (b) Glemser, O.; Filcek, M. *Z. Anorg. Allg. Chem.* **1955**, *279*, 321−323 (c) Gattow, G.; Zemann, J. *Z. Anorg. Allg. Chem.* **1955**, *279*, 324−327.

(7) Voroshilov, Y. V.; Peresh, E. Y.; Golovei, M. I. *Inorg. Mater.* **1972**, *8*, 777−778.

(8) Kanishcheva, A. S.; Mikhailov, J. N.; Lazarev, V. B.; Trippel, A. F. *Dokl. Akad. Nauk, SSSR (Kryst.)* **1980**, *252*, 96−99.

(9) Schmitz, D.; Bronger, W. *Z. Naturforsch.* **1974**, *29b*, 438−439.

(10) Julien-Pouzol, M.; Jaulmes, S.; Laruelle, P. *Acta. Crystallogr.* **1979**, *B35*, 1313−1315.

(11) Aurivillus, B. *Acta Chem. Scand.* **1983**, *A37*, 399−407.

(12) Cordier, G.; Schäfer, H.; Schwidetzky, C. *Rev. Chim. Miner.* **1985**, *22*, 676−683.

(13) Cordier, G.; Schäfer, H.; Schwidetzky, C. *Rev. Chim. Miner.* **1985**, *22*, 631−638.

(14) Volk, K.; Cordier, G.; Cook, R.; Schäfer, H. *Z. Naturforsch.* **1990**, *35b*, 136−140.

(15) Liautard, B.; Garcia, J. C.; Brun, G.; Tedenac, J. C.; Maurin, M. *Eur. J. Solid State Inorg. Chem.* **1990**, *27*, 819−830.

(16) Lee, S.; Fischer, E; Czerniak, J.; Nagasundaram, N. *J. Alloys Comp.* **1993**, *197*, 1−5.

(17) Iitaka, Y.; Nowacki, W. *Acta Crystallogr.* **1962**, *15*, 691−698.

(18) Kupcik, V.; Makovicky, E. *N. Jb. Miner. Mh.* **1968**, *7*, 236−237.

(19) Ohmasa, M.; Nowacki, W. *Z. Kristallogr.* **1973**, *137*, 422−432.

(20) Kohatsu, I; Wuensch, B. J. *Acta Crystallogr.* **1971**, *B27*, 1245−1252.

(21) McCarthy, T. J.; Ngeyi, S.-P.; Liao, J.-H.; DeGroot, D.; Hogan, T.; Kannewurf, C. R.; Kanatzidis, M. G. *Chem. Mater.* **1993**, *5*, 331−340.

(22) McCarthy, T. J.; Tanzer, T. A.; Kanatzidis, M. G. *J. Am. Chem. Soc.* **1995**, *117*, 1294−1301.

(23) (a) Lazarev, V. B.; Trippel', A. F.; Berul', S. I. *Russ. J. Inorg. Chem.* **1977**, *22*, 1218−1220. (b) Trippel', A. F.; Berul', S. I.; Lazarev, V. B. *Russ. J. Inorg. Chem.* **1980**, *25*, 1545−1547. (c) Berul', S. I.; Lazarev, V. B.; Trippel', A. F.; Buchikhina, O. P. **1977**, *22*, 1390−1393. (d) Lazarev, V. B.; Trippel', A. F.; Berul', S. I. *Russ. J. Inorg. Chem.* **1980**, *25*, 1694−1697.

(24) (a) Liao, J.-H.; Varotsis, C.; Kanatzidis, M. G. *Inorg. Chem.*, **1993**, *32*, 2453−2462. (b) Liao, J.-H.; Kanatzidis, M. G., *Chem. Mater.* **1993**, *5*, 1561−1569.

(25) CERIUS: Molecular Simulation Software, Version 3.0, Cambridge Molecular Design, Waltham, MA 02154, 1992.

values for the bandgap in the range 0.5−6.0 eV, which agree rather well with values obtained by absorption measurements from single crystals of the same material.

Differential Thermal Analysis. Differential thermal analysis (DTA) was performed with a computer-controlled Shimadzu DTA-50 thermal analyzer. The ground single crystals (~20.0 mg total mass) were sealed in quartz ampules under vacuum. An quartz ampule containing alumina of equal mass was sealed and placed on the reference side of the detector. The samples were heated to the desired temperature at 10 °C/min and then isothermed for 10 min followed by cooling at 10 °C/min to 100 °C and finally by rapid cooling to room temperature. The reported DTA temperatures are peak temperatures. The DTA samples were examined by powder X-ray diffraction after the experiments.

Charge-Transport Measurements. Dc electrical conductivity and thermopower measurements were made on single crystals and polycrystalline compactions of the compounds. Conductivity measurements were performed in the usual four-probe geometry with 60- and 25-μm gold wires used for the current voltage electrodes, respectively. Measurements of the pellet cross-sectional area and voltage probe separation were made with a calibrated binocular microscope. Conductivity data were obtained with the computer-automated system described elsewhere.[26] Thermoelectric power measurements were made by using a slow ac technique[27] with 60-mm gold wires serving to support and conduct heat to the sample, as well as to measure the voltage across the sample resulting from the applied temperature gradient. In both measurements, the gold electrodes were held in place on the sample with a conductive gold paste.

Conductivity specimens were mounted on interchangeable sample holders, and thermopower specimens were mounted on a fixed sample holder/differential heater. Mounted samples were placed under vacuum (10^{-3} Torr) and heated to room temperature for 2−4 h to cure the gold contacts. For a variable-temperature run, data (conductivity or thermopower) were acquired during both sample cooling and warming to check reversibility. The temperature drift rate during an experiment was kept below 1 K/min. Typically, three to four separate variable-temperature runs were carried out for each sample to ensure reproducibility and stability. At a given temperature, reproducibility was within ±5%.

Thermal Transport Measurements. Thermal conductivity of polycrystalline samples was measured using a steady-state method. Samples were attached to the cold tip of a variable-temperature cryostat with the aid of Stycast epoxy. A small strain-gauge resistor serving as a heater was glued to the other end of the sample. Small crossbars made of flattened 0.25mm diameter copper wire were attached with a tiny amount of Stycast at two positions along the length of a cylindrical sample. The samples were grown as cylindrical polycrystalline ingots from a recrystallization from the melt inside quartz tubes. A pair of calibrated chromel−constantan differential thermocouples (25 μm diameter wires) was soldered to the copper crossbars to measure both the temperature difference ΔT and the temperature of the cold junction. Thermal conductivity was then determined from $K = Ql/S\Delta T$, where Q is the power applied to the heater, l is the spacing between the crossbars, and S is the cross-sectional area of the sample. Measurements were carried out in a vacuum better than 10^{-6} Torr over the temperature range from 4−300 K.

Crystallographic Studies. Both compounds were examined by X-ray powder diffraction for the purpose of phase purity and identification. Accurate d_{hkl} spacings (Å) were obtained from the powder patterns recorded on a Rigaku Rotaflex powder X-ray diffractometer with Ni-filtered Cu Kα radiation operating at 45 kV and 100 mA. The data were collected at a rate of 1.0°/min.

Structure Solution of KBi$_{6.33}$S$_{10}$. A crystal with dimensions 0.02 × 0.05 × 0.25 mm was mounted on a glass fiber. Intensity data were collected using the $\omega-2\theta$ scan mode on a Rigaku AFC6S four-circle automated diffractometer equipped with a graphite-crystal monochromator. The stability of the crystal was monitored by measuring three standard reflections periodically (every 150 reflections) during the course of data collection. No crystal decay was detected. The structure was solved by direct methods using SHELXS86[29a] and refined by full-matrix least-squares techniques of the TEXSAN package of crystallographic programs.[29b] An empirical absorption correction based on ψ scans was applied to the data. Seven bismuth atoms, ten sulfur atoms, and a potassium atom were located on mirror planes. After least-squares refinement, the isotropic temperature factor for Bi(7) was very high at 12.18 Å^2 with $R/R_w = 7.4/9.9$. A refinement of its multiplicity indicated a lower than full occupancy on this site. The occupancy and temperature factor of this atom were refined to give values of 0.263 and 3.945 Å^2, respectively ($R/R_w = 5.7/$ 6.9). The coordination environments of the other six bismuth atoms were octahedral while that of Bi(7) was an unusual eight-coordinate site consisting of bond distances ranging from 2.79 to 3.48 Å. At this stage, a model with bismuth atom vacancies seemed to be reasonable. Since the isotropic temperature factor for Bi(6) was also significantly higher (2.707 Å^2) than those of the other five bismuth atoms (ave = 1.16 Å^2), the occupancy and the temperature factor of Bi(6) were also refined to give values of 0.407 and 1.561 Å^2, respectively ($R/R_w = 5.1/6.0$). The occupancies were fixed at 0.263 (Bi(7)) and 0.407 (Bi(6)). This was in good agreement with the elemental analytical data. DIFABS correction was applied to the isotropically refined data ($R/R_w = 4.8/5.3$).[30] All atoms were refined anisotropically to give a final $R/R_w = 4.3/4.7$. All calculations were performed on a VAXstation 3100/76 computer. As a check for Bi/K disorder, the occupancy of the K site was refined and revealed no change, which suggests that the site is fully occupied with K.

Structure Solution of K$_2$Bi$_8$S$_{13}$. A crystal with dimensions 0.03 × 0.05 × 0.30 mm was mounted on a glass fiber. Intensity data collection and structure solution methods are the same as above. Friedel pairs were collected due to the possibility of an acentric structure. Eight bismuth atoms, thirteen sulfur atoms and two potassium atoms were located on mirror planes. After least-squares refinement, the isotropic temperature factor for Bi(8) was rather high at 6.50 Å^2 with $R/R_w = 13.2/14.3$. The occupancy and temperature factor of this atom were refined to give values of 0.331 and 3.31 Å^2, respectively ($R/R_w = 12.5/13.4$). The coordination environments of the other seven bismuth atoms were octahedral, while that of Bi(8) was the same unusual eight-coordinate site, as seen in KBi$_{6.33}$S$_{10}$, consisting of bond distances ranging from 2.77 to 3.48 Å. The K(1) and K(2) coordination sites were very similar to that of Bi(8). Refinement of the occupancies of K(1) and K(2) showed large increases to 0.815 for K(1) and 0.814 for K(2) (ideal full occupancy should be 0.500). This suggested that more electron density was required at these sites, therefore, a model with Bi and K disordered over all three sites seemed reasonable. Successive refinements, taking into account this hypothesis, resulted in a formula of K$_{2.1}$Bi$_{7.9}$S$_{13}$, where an additional +0.2 charge is needed for electroneutrality ($R/R_w = 12.3/13.0$). The occupancies were rounded off and fixed, and refinement gave K$_2$Bi$_8$S$_{13}$ with no change in the R value. The atomic composition of the Bi-rich site A was found to be 60% Bi and 40% K, while sites B and C gave 20% Bi and 80% K. DIFABS correction was applied to the isotropically refined data ($R/R_w = 7.5/8.5$).[30] All atoms were refined anisotropically except Bi(8), K(1), and K(2) ($R/R_w = 7.3/8.2$). Averaging the data did not affect significantly the R value. K$_2$Bi$_8$S$_{13}$ is found with positional disorder between Bi and K

(26) Lyding, J. W.; Marcy, H. O.; Marks, T. J.; Kannewurf, C. R. *IEEE Trans. Instrum. Meas.* **1988**, *37*, 76−80.

(27) Chaikin, P. I.; Kwak, J. F. *Rev. Sci. Instrum.* **1975**, *46*, 218−220.

(28) Huebener, R. P. *Phys. Rev.* **1964**, *136*, A1740-A1744.

(29) (a) Sheldrick, G. M. In *Crystallographic Computing* 3; Sheldrick, G. M., Kruger, C., Doddard, R., Eds.; Oxford University Press: Oxford, England, 1985; pp 175−189. (b) TEXSAN: Single Crystal Structure Analysis Software, Version 5.0, Molecular Structure Corp., The Woodlands, TX 77381, 1981.

(30) Walker, N.; Stuart, D. *Acta Crystallogr.* **1983**, *A39*, 158−166.

Table 1. Summary of Crystallographic Data and Structure Analysis for KBi$_{6.33}$S$_{10}$ and K$_2$Bi$_8$S$_{13}$[a]

	I	II
formula	KBi$_{6.33}$S$_{10}$	K$_2$Bi$_8$S$_{13}$
FW	1682.54	2166.82
a, Å	24.05(1)	16.818(2)
b, Å	4.100(2)	4.074(5)
c, Å	19.44(1)	17.801(3)
α, deg	90.000	90.000
β, deg	90.000	90.48(1)
γ, deg	90.000	90.000
Z; V, Å^3	4; 1917	2; 1220
λ	0.71073 (Mo Kα)	0.71073 (Mo Kα)
space group	*Pnma* (No. 62)	*P*2$_1$/*m* (No. 11)
D_{calc}, g/cm^3	5.828	5.900
μ, cm^{-1}	590 (Mo Kα)	588 (Mo Kα)
$2\theta_{max}$, deg	50	50
temp, °C	23	23
final R/R_w, %	4.3/4.7	7.3/8.2
total data measd	2015	3888
total unique data	2015	1944
data with $F_o^2 > 3\sigma(F_o^2)$	862	1924 (averaged)
no. of variables	108	131

[a] $R = \sum(|F_o| - |F_c|)/\sum|F_o|$, $R_w = \{\sum w(|F_o| - |F_c|)^2/\sum w|F_o|^2\}^{1/2}$. The reflections were weighted according to $w = 1/[\sigma(F_o^2)^2 + (0.03F_o^2)^2]^{1/2}$ (where w = weight of a given F_o).

Table 2. Fractional Atomic Coordinates and B_{eq} Values for KBi$_{6.33}$S$_{10}$ with Estimated Standard Deviations in Parentheses

atom	x	y	z	B_{eq},[a] Å^2
Bi(1)	0.2995(1)	0.25	0.0913(1)	1.2(1)
Bi(2)	0.17185(9)	0.75	0.1898(1)	1.3(1)
Bi(3)	0.4327(1)	0.75	0.0364(1)	1.5(1)
Bi(4)	0.0435(1)	0.25	0.2754(1)	1.6(1)
Bi(5)	0.1502(1)	0.25	−0.0143(1)	2.0(1)
Bi(6)[b]	0.5090(1)	0.75	0.4015(1)	1.6(1)
Bi(7)[c]	0.2219(3)	0.25	0.3830(3)	4.0(3)
K	0.3705	0.25	0.2834(8)	2.6(7)
S(1)	0.0878(6)	0.25	0.1390(9)	2.4(8)
S(2)	0.2227(7)	0.75	0.0332(8)	2.3(8)
S(3)	0.3594(6)	0.75	0.1482(7)	1.9(7)
S(4)	0.5000	0.25	0.0897(8)	1.9(7)
S(5)	0.2375(6)	0.25	0.2294(7)	1.7(7)
S(6)	0.4732(5)	0.75	0.2716(7)	1.5(6)
S(7)	0.4287(8)	0.25	0.4452(8)	3.0(8)
S(8)	0.3621(6)	0.25	−0.0166(7)	1.6(7)
S(9)	0.6227(6)	0.75	0.1930(8)	1.5(7)
S(10)	0.7998(7)	0.75	0.1299(7)	2.0(7)

[a] B values for anisotropically refined atoms are given in the form of the isotropic equivalent displacement parameters defined as $B_{eq} = \frac{4}{3}[a^2B(1,1) + b^2B(2,2) + c^2B(3,3) + ab(\cos \gamma)B(1,2) + ac(\cos \beta)B(1,3) + bc(\cos \alpha)B(2,3)]$. [b] This site is 81% occupied. [c] This site is 53% occupied.

with a bias toward K$_{2.1}$Bi$_{7.9}$S$_{13}$, suggesting a Bi^{3+} or K$^+$ deficiency. Nonstoichiometry represented by K$_{2+3x}$Bi$_{8-x}$S$_{13}$ could be present.

The complete data collection parameters, details of the structure solution and refinement and for both compounds are given in Table 1. The coordinates and average temperature factors (B_{eq}) of all atoms and their estimated standard deviations for both compounds are given in Tables 2 and 3.

Results and Discussion

Synthesis, Spectroscopy, and Thermal Analysis. The synthesis of pure KBi$_{6.33}$S$_{10}$ can be accomplished by reacting K$_2$S and Bi$_2$S$_3$ (1.0:3.3) at 800 °C. Pure K$_2$Bi$_8$S$_{13}$ can be obtained with a ratio of 1.0:4.0 at 750 °C. The known ternary phase, α-KBiS$_2$,[6] was obtained as a pure phase by reacting K$_2$S and Bi$_2$S$_3$ (1:1) at 725 °C. Surprisingly, instead of α-KBiS$_2$, β-KBiS$_2$ was observed as the major product in the reaction of K$_2$S and Bi$_2$S$_3$

Table 3. Fractional Atomic Coordinates and B_{eq} Values for K$_2$Bi$_8$S$_{13}$ with Estimated Standard Deviations in Parentheses

atom	x	y	z	B_{eq},[a] Å^2
Bi(1)	0.9176(1)	0.25	0.5774(1)	1.27(9)
Bi(2)	1.1729(1)	0.25	0.6245(1)	1.3(1)
Bi(3)	0.6731(1)	0.25	0.5194(1)	1.3(1)
Bi(4)	0.8930(1)	−0.75	0.9783(1)	1.4(1)
Bi(5)	0.6929(1)	−0.25	0.9550(1)	1.3(1)
Bi(6)	1.0134(1)	−0.25	0.7540(1)	1.4(1)
Bi(7)	0.4917(1)	−1.75	0.8849(1)	1.5(1)
Bi(8)(K)[b]	0.2908(3)	−2.25	0.8195(3)	3.5(1)
K(1)(Bi)[c]	0.7268(7)	−2.25	0.7188(8)	3.0(3)
K(2)(Bi)[c]	0.5219(8)	−1.25	0.6542(8)	3.0(3)
S(1)	0.978(1)	−0.25	0.9073(9)	2.0(7)
S(2)	0.8982(8)	0.25	0.7227(8)	1.2(6)
S(3)	0.8082(8)	−0.25	0.559(1)	1.8(7)
S(4)	0.3889(9)	−1.75	0.7739(9)	1.8(7)
S(5)	0.807(1)	−1.25	1.0574(9)	1.8(7)
S(6)	0.7676(8)	−0.75	0.8767(7)	1.5(6)
S(7)	1.0418(8)	−0.75	0.5966(8)	1.5(6)
S(8)	1.131(1)	−0.75	0.7654(9)	1.7(6)
S(9)	0.629(1)	−1.75	0.661(1)	2.3(8)
S(10)	0.5784(7)	−0.25	0.4890(9)	1.5(6)
S(11)	0.573(1)	−1.25	0.820(1)	2.5(8)
S(12)	0.7258(8)	0.25	0.352(1)	1.7(7)
S(13)	0.610(1)	0.25	0.039(1)	2.7(8)

[a] B values for anisotropically refined atoms are given in the form of the isotropic equivalent displacement parameters defined as $B_{eq} = \frac{4}{3}[a^2B(1,1) + b^2B(2,2) + c^2B(3,3) + ab(\cos \gamma)B(1,2) + ac(\cos \beta)B(1,3) + bc(\cos \alpha)B(2,3)]$. [b] This site contains 60% Bi and 40% K. [c] This site contains 80% K and 20% Bi.

Table 4. High-Temperature K$_2$S/Bi$_2$S$_3$ Reactions

K$_2$S	Bi$_2$S$_3$	temp (°C)	product
1	3.0	800	KBi$_{6.33}$S$_{10}$
1	3.3	800	KBi$_{6.33}$S$_{10}$
1	3.5	800	KBi$_{6.33}$S$_{10}$
1	4.0	750	K$_2$Bi$_8$S$_{13}$
1	4.0	800	K$_2$Bi$_8$S$_{13}$
1	4.4	800	K$_2$Bi$_8$S$_{13}$
1	5.0	800	K$_2$Bi$_8$S$_{13}$/Bi$_2$S$_3$
1	6.0	800	K$_2$Bi$_8$S$_{13}$/Bi$_2$S$_3$
1	6.33	785	K$_2$Bi$_8$S$_{13}$/Bi$_2$S$_3$
1	6.80	800	K$_2$Bi$_8$S$_{13}$/Bi$_2$S$_3$

(1:2) at 725 °C along with KBi$_{6.33}$S$_{10}$ as a minor product. β-KBiS$_2$ is isostructural to RbBiS$_2$[7] in which CdCl$_2$-type (BiS$_2$)$^-$ layers (perpendicular to the c axis) alternate with Rb$^+$ ions. Three (BiS$_2$)$^-$ layers are found in the unit cell of this compound. The coordination sphere of Bi is nearly perfect octahedral. Increasing the amount of Bi$_2$S$_3$ to 1:3 resulted in the formation of KBi$_{6.33}$S$_{10}$. The results of several direct combination reactions are shown in Table 4.

KBi$_{6.33}$S$_{10}$, K$_2$Bi$_8$S$_{13}$, and β-KBiS$_2$ belong to the (A$_2$Q)$_n$-(Bi$_2$Q$_3$)$_m$ (A = alkali metal; Q = S, Se) general family of compounds with $n = 1$ and $m = 6.33$, 4, and 1, respectively. The synthesis of new ternary bismuth chalcogenides with various n and m values may be possible, e.g., ABi$_5$Q$_8$ ($n = 1$, $m = 5$).

The optical properties of I and K$_2$Bi$_8$S$_{13}$ were assessed by studying the UV−visible−near-IR reflectance spectra of the materials. The compounds absorbed all light in the range 0.5−6.2 eV. The spectra confirm that the bandgaps, E_g, of these two compounds are less than 0.5 eV (the detection limit of the instrument). Diffuse reflectance infrared spectroscopy was used to probe the small bandgap of the compounds. The absorption edges in both compounds were found to be virtually identical in the range of 0.06−0.25 eV (see Figure 1). The narrow bandgaps for KBi$_{6.33}$S$_{10}$ and K$_2$Bi$_8$S$_{13}$ could result from
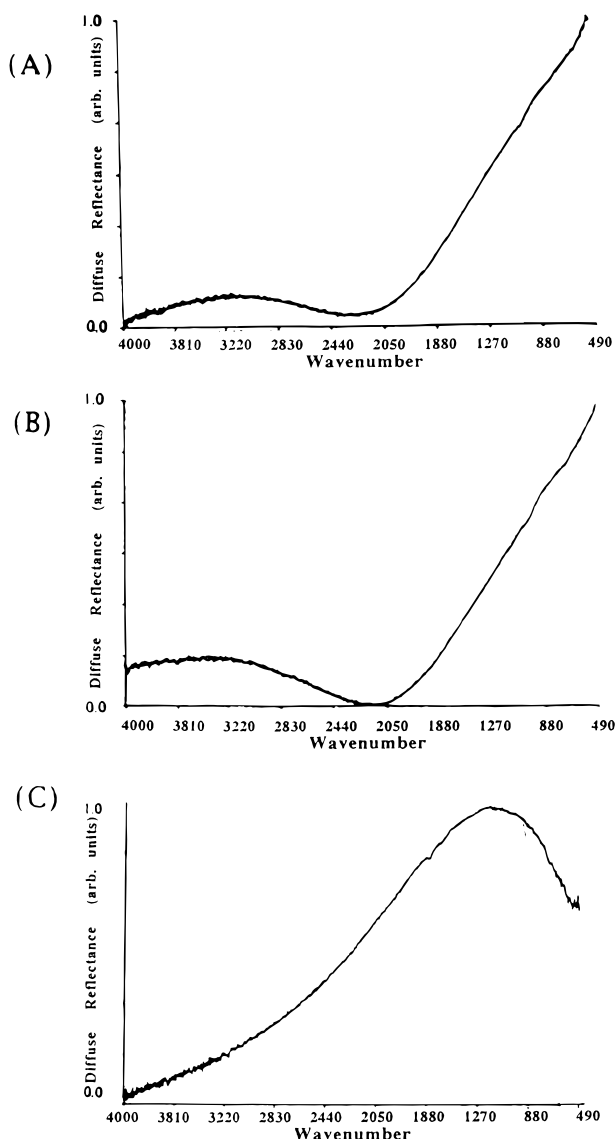
Figure 1. Infrared diffuse reflectance spectra of (a) $KBi_{6.33}S_{10}$ and (b) $K_2Bi_8S_{13}$. (c) For comparison, the mid-IR diffuse reflectance spectrum of Bi_2Se_3 ($E_g = 0.33$ eV) is shown.

the existence of a narrow dopant level band just below the conduction band.

The thermal behavior of the two compounds was investigated with differential thermal analysis (DTA, see Figure 2). Both $KBi_{6.33}S_{10}$ and $K_2Bi_8S_{13}$ melt congruently at 710 and 713 °C as evidenced by powder XRD. Multiple heating/cooling cycles confirmed the thermal stability of these compounds.

Description of Structures. Structure of $KBi_{6.33}S_{10}$. This compound has a three-dimensional structure made up of Bi_2Te_3-type (NaCl-type) blocks and CdI_2-type fragments that connect to form tunnels filled with eight-coordinate K^+ cations ($K-S_{ave} = 3.3(1)$ Å). Selected bond distances and angles for **I** are given in Tables 5 and 6. Figure 3 shows the packing diagram of the extended structure down the *b* axis. The $[Bi_{6.33}S_{10}]^-$ framework is made of edge-sharing BiS_6 octahedra, as shown in Figure 4. In an architectural context, it can be thought of as an intimate composite of two different layered structure types interconnected to form a 3-D network. Structural features from the NaCl and CdI_2[31] lattices are represented in this framework. The features derived from both these fundamen-
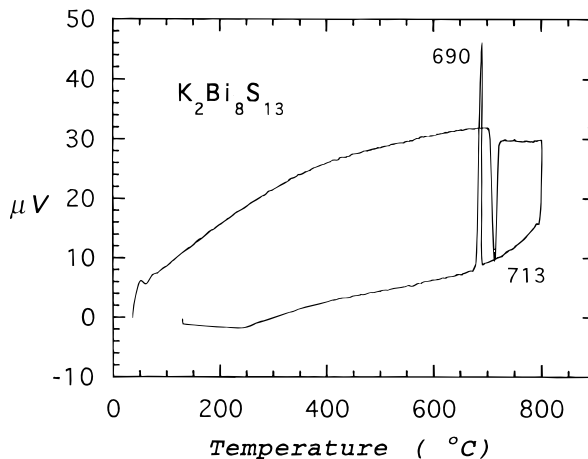
Figure 2. Typical DTA diagram of $K_2Bi_8S_{13}$. $KBi_{6.33}S_{10}$ gives a similar diagram.

Table 5. Selected Distances (Å) in $KBi_{6.33}S_{10}$ with Standard Deviations in Parentheses[a]

Bi(1)−S(2)	2.98(1)	Bi(5)−S(1)	3.34(2)
Bi(1)−S(2′)	2.98(1)	Bi(5)−S(2)	2.84(1)
Bi(1)−S(3)	2.74(1)	Bi(5)−S(2′)	2.84(1)
Bi(1)−S(3′)	2.74(1)	Bi(5)−S(7′)	2.90(1)
Bi(1)−S(5)	3.07(1)	Bi(5)−S(7″)	2.90(1)
Bi(1)−S(8)	2.58(1)	Bi(5)−S(10)	2.55(1)
Bi(1)−S (mean)	2.8(2)	Bi(5)−S (mean)	2.9(3)
Bi(2)−S(1)	3.04(1)	Bi(6)−S(1)	2.90(1)
Bi(2)−S(1′)	3.04(1)	Bi(6)−S(1″)	2.90(1)
Bi(2)−S(2)	3.28(2)	Bi(6)−S(6)	2.67(1)
Bi(2)−S(5)	2.70(1)	Bi(6)−S(7)	2.94(1)
Bi(2)−S(5′)	2.70(1)	Bi(6)−S(7‴)	2.94(1)
Bi(2)−S(9)	2.57(2)	Bi(6)−S(7⁗)	3.34(2)
Bi(2)−S (mean)	2.9(3)	Bi(6)−S (mean)	2.9(2)
Bi(3)−S(3)	2.80(1)	Bi(7)−S(2″)	3.21(2)
Bi(3)−S(4)	2.810(6)	Bi(7)−S(5)	3.01(2)
Bi(3)−S(4′)	2.810(6)	Bi(7)−S(8)	3.48(1)
Bi(3)−S(4″)	2.94(1)	Bi(7)−S(8′)	3.48(1)
Bi(3)−S(8)	2.85(1)	Bi(7)−S(9′)	3.47(1)
Bi(3)−S(8′)	2.85(1)	Bi(7)−S(9)	3.47(1)
Bi(3)−S (mean)	2.84(5)	Bi(7)−S(10′)	2.79(1)
		Bi(7)−S(10″)	2.79(1)
Bi(4)−S(1)	2.86(2)	Bi(7)−S (mean)	3.2(3)
Bi(4)−S(4‴)	2.82(1)		
Bi(4)−S(6′)	2.812(9)	K−S(3)	3.34(2)
Bi(4)−S(6″)	2.812(9)	K−S(3′)	3.34(2)
Bi(4)−S(9′)	2.86(1)	K−S(5)	3.37(2)
Bi(4)−S(9)	2.86(1)	K−S(6)	3.22(1)
Bi(4)−S (mean)	2.84(3)	K−S(6‴)	3.22(1)
		K−S(7)	3.44(2)
		K−S(10′)	3.15(1)
		K−S(10″)	3.15(1)
		K−S (mean)	3.3(1)

[a] The estimated standard deviations in the mean bond lengths and the mean bond angles are calculated by the equations $\sigma l = \{\sum_n (l_n - l)^2/n(n-1)\}^{1/2}$, where l_n is the length (or angle) of the *n*th bond, *l* the mean length (or angle), and *n* the number of bonds.

tal structure types found in the $[Bi_{6.33}S_{10}]^-$ framework are highlighted in Figure 5. The NaCl-type rod-shaped fragments are linked by rod-shaped CdI_2-type blocks to form the channel framework. The two different fragments are joined via high coordinate Bi atoms (i.e., Bi-(7)), in the same way it is found in mineral sulfo salts.[32] Another interesting feature found in this structure is

(31) Mitchell, R. S. *Z. Kristallogr.* **1956**, *108*, 296−315.

(32) (a) Makovicky, E., *Eur. J. Mineral.* **1993**, *5*, 545−591 (b) Makovicky, E. *Fortschr. Miner.* **1981**, *59*, 137−190. (c) Makovicky, E. *Neues Jahrbuch Miner. Abh.* **1989**, *160*, 269−297.

Table 6. Selected Angles (deg) in $KBi_{6.33}S_{10}$ with Standard Deviations in Parentheses

S(2)−Bi(1)−S(2′)	86.9(4)	S(2)−Bi(5)−S(2′)	92.2(5)
S(2)−Bi(1)−S(3)	88.0(4)	S(2)−Bi(5)−S(7″)	88.8(3)
S(3)−Bi(1)−S(3′)	96.9(5)	S(2)−Bi(5)−S(10)	89.8(4)
S(3)−Bi(1)−S(8)	91.3(4)	S(7′)−Bi(5)−S(7″)	89.9(5)
S(1)−Bi(2)−S(1′)	84.7(4)	S(1)−Bi(6)−S(1″)	89.9(5)
S(1)−Bi(2)−S(5)	88.3(3)	S(1)−Bi(6)−S(6)	87.3(4)
S(1)−Bi(2)−S(9)	89.0(4)	S(6)−Bi(6)−S(7)	93.5(4)
S(5)−Bi(2)−S(9)	90.9(4)	S(7)−Bi(6)−S(7‴)	88.4(5)
S(3)−Bi(3)−S(4)	94.4(3)	S(5)−Bi(7)−S(10′)	80.0(4)
S(3)−Bi(3)−S(8)	84.6(4)	S(5)−Bi(7)−S(10″)	80.0(4)
S(4)−Bi(3)−S(4′)	93.7(3)	S(10′)−Bi(7)−S(10″)	94.6(5)
S(4)−Bi(3)−S(8)	87.2(2)	S(2″)−Bi(7)−S(5)	148.3(5)
S(1)−Bi(4)−S(6′)	85.5(4)		
S(1)−Bi(4)−S(9)	87.2(4)		
S(4)−Bi(4)−S(6′)	94.5(3)		
S(4)−Bi(4)−S(9)	92.7(3)		

the presence of small triangular-shaped empty channels that are lined by Bi(7)−S(8)−Bi(4)−S(4)−Bi(3)−S(9). The same type of channels has been observed in β-$BaBi_2S_4$.[11]

The existence of Bi_2Te_3- and CdI_2-type fragments, with Bi in an octahedral coordination site, is a common structural motif that runs through much of the known bismuth chalcogenide chemistry. The structure of $CsBi_3S_5$[8] is comprised of Bi_2Te_3-type single chains that run along the *b* direction and share corners in the *a*−*c* plane to form a three-dimensional tunnel structure filled with Cs^+ ions. In $Cs_3Bi_7Se_{12}$,[12] the $[Bi_7Se_{12}]^{3-}$ anions are slabs. They contain CdI_2- and Bi_2Te_3-type fragments that connect in an edge-sharing manner to form a lamellar structure. In $Sr_4Bi_6Se_{13}$,[13] the highly charged $[Bi_6Se_{13}]^{8-}$ anion has a very interesting structure. It contains two-dimensional sheets made up of edge-sharing CdI_2- and Bi_2Te_3-type fragments. One-dimensional double chains, comprised of Bi_2Te_3-type blocks, extend along the *b* direction and separate these layers. In $BaBiSe_3$[14] and in $BaBiTe_3$[33] one-dimensional single chains, comprised of Bi_2Te_3-type blocks, are linked by unusual zig-zag $(Se_x)^{x-}$ and $(Te_x)^{x-}$ chains respectively to form a layered structure.

Atoms Bi(3,4) possess only slightly distorted octahedral coordination with Bi−S bond distances ranging from 2.80(1) to 2.94(1) Å for Bi(3) and 2.812(9) to 2.86-(1) Å for Bi(4). These distances are similar to those reported in $CsBi_3S_5$ (Bi3).[8] In contrast, the octahedral coordination environments in Bi(1), Bi(2), Bi(5), and Bi-(6) are highly distorted with a short bond that is trans to a long bond (Figure 6). This type of coordination environment is very prevalent in bismuth chalcogenide chemistry and results from the influence of the non-bonded, stereochemically active $6s^2$ electron lone pair. For example, the Bi(2)−S(9) bond distance of 2.57(2) Å is *trans* to a long Bi(2)−S(1) distance of 3.28(2) Å. This same type of distorted octahedral coordination, bordering on square-pyramidal coordination, is found in many compounds including $CsBi_3S_5$ (Bi1,2),[8] $Tl_4Bi_2S_5$,[10] and α-(β-)$BaBi_2S_4$.[11] The sites of Bi(6) and Bi(7) are partially occupied at 81% and 53%, respectively. Bi(7) possesses a distorted seesaw structure or a trigonal-bipyramidal coordination if one includes the lone pair, with four normal Bi−S bonds ranging from 2.79(1) to 3.21(2) Å. The lone pair is directed at four squarely arranged
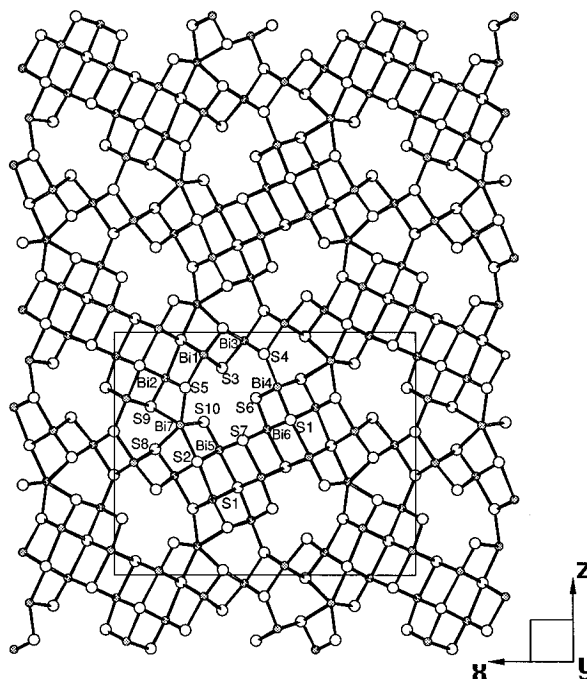
---

(33) Chung, D. Y.; Kanatzidis M. G., manuscript in preparation.

Figure 3. Extended framework in $KBi_{6.33}S_{10}$ down the *b* axis with labeling. The potassium atoms are omitted for clarity.
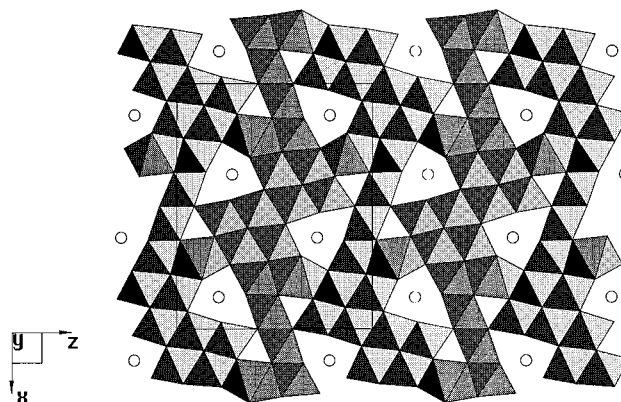

Figure 4. Polyhedral representation of $KBi_{6.33}S_{10}$ down the *b* axis showing the connectivity of the BiS_6 octahedra. The potassium atoms are the open circles.

sulfur atoms with long Bi−S distances of 3.47(1) and 3.48(1) Å. The axial S(2″)−Bi(7)−S(5) angle is much less than 180° at 148.3(5)°, and the equatorial S(10′)−Bi(7)−S(10″) angle is 94.5(5)°. These angles are influenced by the stereochemically active lone pair. If the four sulfur atoms (i.e., S(9), S(9), S(8), and S(8)) are included in the coordination sphere of Bi(7), then the overall polyhedron becomes a bicapped trigonal prism (see Figure 6).

Structure of $K_2Bi_8S_{13}$. This compound also possesses a three-dimensional structure made up of NaCl or Bi_2Te_3- and CdI_2-type rod-shaped fragments that connect to form a structure with tunnels. Here too, the highly coordinated Bi(8) atoms serve to stitch the rods together. The K^+ cations are disordered with one of the Bi^{3+} ions over three distinct crystallographic sites. This, although not expected, can be rationalized by the similar sizes of K^+ and Bi^{3+}. This structure is quite different from that of its selenium analogue $K_2Bi_8Se_{13}$.[21] Selected bond distances and angles for $K_2Bi_8S_{13}$ are given in Tables 7 and 8.
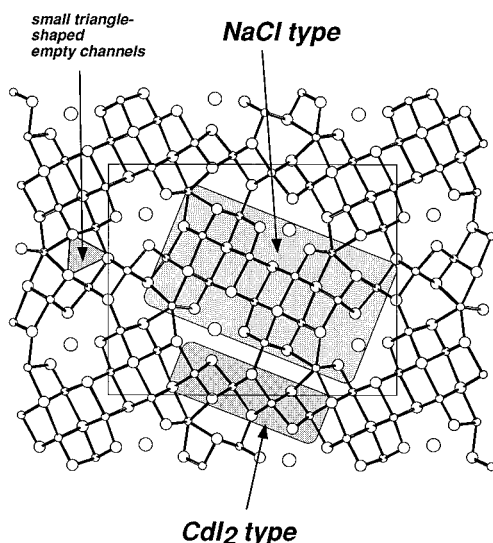
Figure 5. Projections of the structure of $[Bi_{6.33}S_{10}]^-$ framework. Both the NaCl and the CdI_2 structure types are found in this framework as highlighted by the shaded areas.

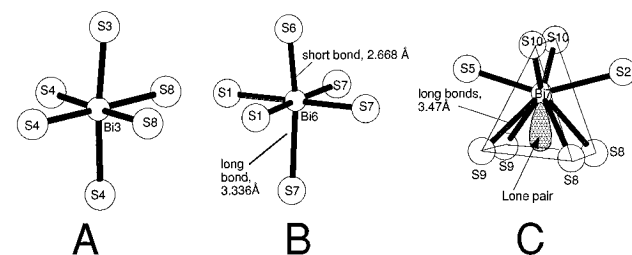**Figure 6.** Three different kinds of Bi polyhedra found in $KBi_{6.33}S_{10}$: (A) an only slightly distorted octahedron, (B) a highly distorted octahedron, and (C) the highly coordinated Bi(7) in a bicapped prismatic geometry. For Bi−S distance and S−Bi−S angles see Tables 5 and 6.

Figure 7 shows the extended $[Bi_8S_{13}]^{2-}$ framework down the *b* axis. As in $KBi_{6.33}S_{10}$, this framework is based on structural features from the Bi_2Te_3 and CdI_2 lattices and contains the small triangular-shaped empty channels. The tunnels of $K_2Bi_8S_{13}$, which can be better viewed in Figure 8, are more open than those of $KBi_{6.33}S_{10}$ because more K_2S is present per formula unit. $K_2Bi_8S_{13}$ can be viewed as a derivative of the well-known Bi_2S_3 compound generated by breaking down the Bi_2S_3 framework by incorporation of K_2S in the molar ratio of 1:4 (i.e., $[K_2S][Bi_2S_3]_4$). The corresponding $[K_2S]/[Bi_2S_3]$ ratio in $KBi_{6.33}S_{10}$ is 1:6.33, so less K^+ ions are present resulting in smaller channels.

Bi(4) and Bi(6) possess regular octahedral coordination with Bi−S bond distances ranging from 2.77(1) to 2.96(2) Å for Bi(4) and 2.80(2) to 2.86(1) Å for Bi(6). As in $KBi_{6.33}S_{10}$, the octahedral coordination environments of Bi(1), Bi(2), Bi(3), Bi(5), and Bi(7) are distorted with a short bond that is trans to a long bond but with normal octahedral angles, (Figure 9). For example, the Bi(2)−S(8) bond distance of 2.61(2) Å is trans to a long Bi(2)−S(3″) distance of 3.29(2) Å.

Bi(8) is disordered over three sites with K(1,2). The Bi(8) site contains approximately 60% Bi and 40% K, while the other two sites contain mainly K (~80%). Bi-(8) possesses the same type of distorted bicapped trigonal prismatic as found for Bi(7) (in $KBi_{6.33}S_{10}$), with four normal Bi−S bonds ranging from 2.75(1) to 3.06(2) Å and four longer distances from 3.43(1) to 3.50(1) Å.[34]

Table 7. Selected Distances (Å) in $K_2Bi_8S_{13}$ with Standard Deviations in Parentheses[a]

Bi(1)−S(2)	2.61(1)	Bi(6)−S(7)	2.84(2)
Bi(1)−S(3)	2.764(9)	Bi(6)−S(8)	2.84(1)
Bi(1)−S(3′)	2.764(9)	Bi(6)−S(8′)	2.84(1)
Bi(1)−S(7)	2.93(1)	Bi(6)−S(mean)	2.84(2)
Bi(1)−S(7′)	2.93(1)		
Bi(1)−S(7″)	3.18(2)	Bi(7)−S(4)	2.61(1)
Bi(1)−S(mean)	2.9(2)	Bi(7)−S(11)	2.71(1)
		Bi(7)−S(11‴)	2.71(1)
Bi(2)−S(3″)	3.29(2)	Bi(7)−S(13″)	3.38(2)
Bi(2)−S(7)	3.04(1)	Bi(7)−S(13‴)	2.99(1)
Bi(2)−S(7′)	3.04(1)	Bi(7)−S(13⁗)	2.99(1)
Bi(2)−S(8)	2.61(2)	Bi(7)−S(mean)	2.9(3)
Bi(2)−S(12′)	2.688(9)		
Bi(2)−S(12″)	2.688(9)	Bi(8)−S(4)	2.75(1)
Bi(2)−S(mean)	2.9(3)	Bi(8)−S(4′)	2.75(1)
		Bi(8)−S(5″)	3.43(1)
Bi(3)−S(3)	3.13(1)	Bi(8)−S(5‴)	3.43(1)
Bi(3)−S(3′)	3.13(1)	Bi(8)−S(8″)	3.50(1)
Bi(3)−S(9′)	2.63(2)	Bi(8)−S(8‴)	3.50(1)
Bi(3)−S(10)	2.639(8)	Bi(8)−S(12‴)	3.06(2)
Bi(3)−S(10′)	2.639(8)	Bi(8)−S(13‴)	3.01(2)
Bi(3)−S(12)	3.12(2)	Bi(8)−S(mean)	3.2(3)
Bi(3)−S(mean)	2.9(3)		
		K(1)−S(2″)	3.53(1)
Bi(4)−S(1)	2.80(1)	K(1)−S(2‴)	3.53(1)
Bi(4)−S(1′)	2.80(1)	K(1)−S(3″)	3.16(2)
Bi(4)−S(1″)	2.96(2)	K(1)−S(6″)	3.54(2)
Bi(4)−S(5)	2.87(1)	K(1)−S(6‴)	3.54(2)
Bi(4)−S(5′)	2.87(1)	K(1)−S(9)	2.81(1)
Bi(4)−S(6)	2.77(1)	K(1)−S(9″)	2.81(1)
Bi(4)−S(mean)	2.85(7)	K(1)−S(11‴)	3.17(2)
		K(1)−S(mean)	3.3(3)
Bi(5)−S(5′)	2.64(2)		
Bi(5)−S(6)	2.78(1)	K(2)−S(4)	3.71(1)
Bi(5)−S(6′)	2.78(1)	K(2)−S(4″)	3.71(1)
Bi(5)−S(11″)	3.12(2)	K(2)−S(9)	2.72(1)
Bi(5)−S(13)	2.89(1)	K(2)−S(9‴)	2.72(1)
Bi(5)−S(13′)	2.89(1)	K(2)−S(10′)	3.10(2)
Bi(5)−S(mean)	2.9(2)	K(2)−S(10‴)	3.66(1)
		K(2)−S(10⁗)	3.66(1)
Bi(6)−S(1)	2.80(2)	K(2)−S(11)	3.07(2)
Bi(6)−S(2)	2.86(1)	K(2)−S(mean)	3.3(4)
Bi(6)−S(2′)	2.86(1)		

[a] The estimated standard deviations in the mean bond lengths and the mean bond angles are calculated by the equations $\sigma l = \{\sum_n(l_n - l)^2/n(n - 1)\}^{1/2}$, where l_n is the length (or angle) of the *n*th bond, *l* the mean length (or angle), and *n* the number of bonds.

Table 8. Selected Angles (deg) in $K_2Bi_8S_{13}$ with Standard Deviations in Parentheses

S(2)−Bi(1)−S(3)	91.6(4)	S(5′)−Bi(5)−S(6)	91.0(4)
S(2)−Bi(1)−S(7)	88.8(4)	S(5′)−Bi(5)−S(13)	89.6(4)
S(3)−Bi(1)−S(3′)	95.0(4)	S(6)−Bi(5)−S(6′)	94.4(4)
S(3)−Bi(1)−S(7)	88.6(3)	S(13)−Bi(5)−S(13′)	89.6(5)
S(3″)−Bi(2)−S(7)	85.1(3)	S(1)−Bi(6)−S(8)	94.7(4)
S(3″)−Bi(2)−S(12)	95.2(4)	S(2)−Bi(6)−S(7)	85.8(3)
S(7)−Bi(2)−S(8)	87.4(4)	S(2)−Bi(6)−S(8′)	88.5(3)
S(8)−Bi(2)−S(12′)	91.4(4)	S(7)−Bi(6)−S(8)	87.0(4)
S(3)−Bi(3)−S(3′)	81.3(3)	S(4)−Bi(7)−S(11)	90.7(4)
S(3)−Bi(3)−S(9)	89.7(4)	S(4)−Bi(7)−S(13‴)	88.0(4)
S(9′)−Bi(3)−S(10)	91.2(4)	S(11)−Bi(7)−S(13⁗)	88.4(4)
S(10)−Bi(3)−S(12)	88.8(4)	S(13″)−Bi(7)−S(13‴)	88.2(4)
S(1)−Bi(4)−S(1′)	93.4(5)	S(4)−Bi(8)−S(4′)	95.7(5)
S(1)−Bi(4)−S(6)	95.5(4)	S(4)−Bi(8)−S(5″)	157.4(4)
S(5)−Bi(4)−S(5′)	90.4(4)	S(4)−Bi(8)−S(12″)	75.9(4)
S(5)−Bi(4)−S(6)	86.4(4)	S(5‴)−Bi(8)−S(12)	126.7(3)

The corners of the prism are defined by atoms S4, S5, S8 and their symmetry-equivalent ones, while the capping atoms are S12 and S13 (see Figure 9). The presence of these high coordination sites seems necessary in stabilizing these structures. The two K sites have distances ranging from 2.81(1) to 3.54(2) Å for K(1)
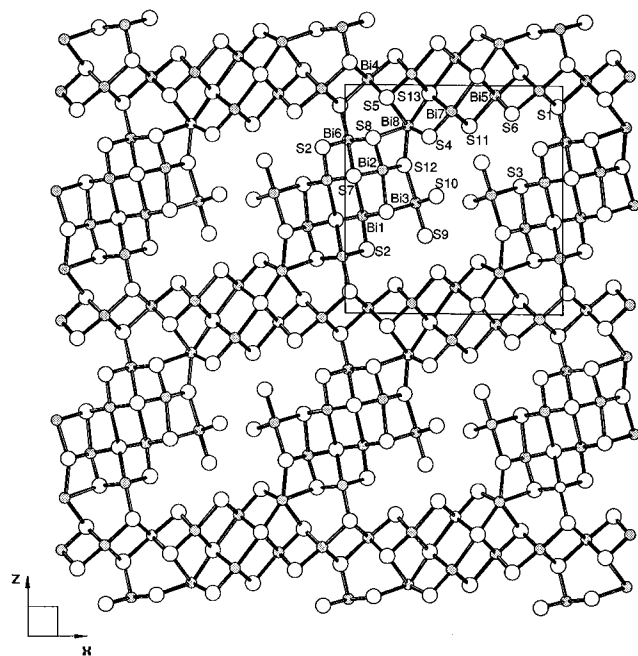
Figure 7. Extended framework in $K_2Bi_8S_{13}$ viewed down the *b* axis with labeling. The potassium atoms are omitted for clarity.
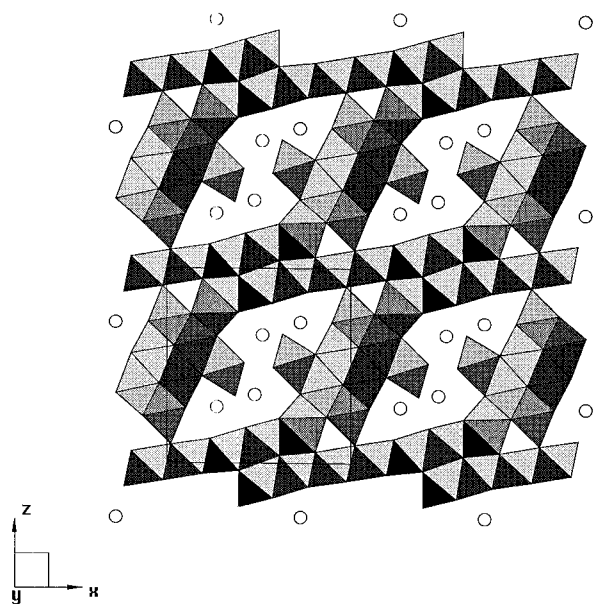

Figure 8. Polyhedral representation of $K_2Bi_8S_{13}$ down the *b* axis showing the connectivity of the BiS_6 octahedra. The potassium atoms are the open circles.

and 2.72(2) to 3.66(2) Å for K(2). These distances are similar to those found for the predominantly Bi(8) site. The K−S distances below 3.0 Å are unusual and presumably a result of averaging over the mixed K/Bi sites. Since the Bi(8) and the potassium sites have similar coordination characteristics and similar pocket sizes, it is not surprising, after all, that a site occupancy

---

(34) Close examination of the known ternary Bi/Q compounds reveals an interesting trend. The esd's of the Bi−S and Bi−Se bond lengths are quite high for such structures. For example, values for $KBi_{6.33}S_{10}$ and $K_2Bi_8S_{13}$ range from 0.006 to 0.02. Other bismuth chalcogenide crystal structures show high esd's for these bonds as follows $CsBi_3S_5$ (0.01),[8] $Tl_4Bi_2S_5$ (0.01−0.02),[10] α-(β-)$BaBi_2S_4$ (0.01−0.03),[11] $Cs_3Bi_7Se_{12}$ (0.011),[12] $Sr_4Bi_6Se_{13}$ (0.011),[13] $BaBiSe_3$ (0.014),[14] and β-$CsBiS_2$ (0.008−0.01).[21] As the diffracting quality of these crystals seems quite good, no obvious explanation for this has been advanced.
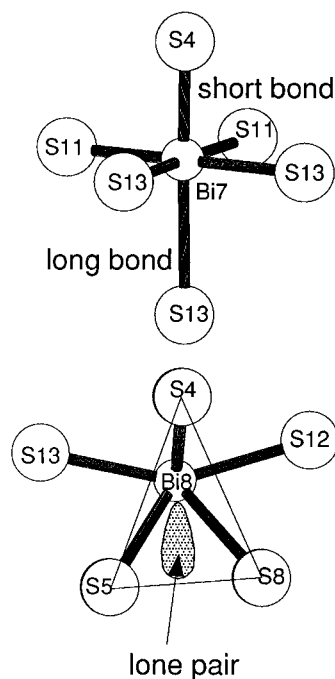

Figure 9. Top: typical highly distorted octahedron (representative of Bi(1), Bi(2), Bi(3), Bi(5), and Bi(7) in $K_2Bi_8S_{13}$. Bottom: the highly coordinated Bi(8) in a bicapped prismatic geometry. For Bi−S distance and S−Bi−S angles see Tables 7 and 8.

exchange exists between these ions. To the best of our knowledge, there are no known systems that have alkali metal/Bi disorder. The closest example is $Cu_{1+3x}Bi_{5-x}S_8$,[15] where Cu^+ and Bi^{3+} ions are disordered over one site.

Electrical Conductivity and Thermoelectric Power Measurements. Four-probe electrical conductivity measurements on polycrystalline chunks of $KBi_{6.33}S_{10}$ showed that the material is a semiconductor with room temperature conductivity $\sigma \sim 10^2$ S/cm which drops to 10^{-4} S/cm at 5 K. Figure 10a shows the log conductivity vs temperature plot for $KBi_{6.33}S_{10}$. The data can be fit to the equation shown below suggesting an activation energy of $E_a = 0.045$ eV:

$$\sigma = \sigma e^{-E_a/k_B T}$$

Figure 10b shows the log conductivity as a function of temperature for $K_2Bi_8S_{13}$. The conductivity of $\sim 10^2$ S/cm (room temperature) and the weak temperature dependence between 5 and 300 K coupled with the IR optical data (vide supra) suggests that this compound is a semi-metal or a narrow-bandgap semiconductor. It is noteworthy that the conductivity of both these ternary compounds is significantly higher than that of the parent Bi_2S_3. The latter possesses a much higher bandgap of 1.1 eV. The conductivity of $\sim 10^2$ S/cm is compared to the values of other semi-metals such as Bi_2Te_3 (2.2×10^3 S/cm)[35] and Bi_2Se_3 ($(1.6-2.0) \times 10^3$ S/cm, Bi_2Te_3-type)[36] obtained from single crystals of these materials.

The conductivity measurements alone cannot unequivocally characterize the electrical behavior of $KBi_{6.33}S_{10}$ and $K_2Bi_8S_{13}$. A complementary probe to address this issue is thermoelectric power (TP) mea-

---

(35) Rosi, F. D.; Abeles, B.; Jengen, R. V. *J. Phys. Chem. Solids* **1959**, *10*, 191.

(36) Black, J.; Conwell, E. M.; Seigle, L.; Spencer, C. W. *J. Phys. Chem. Solids* **1957**, *2*, 240.
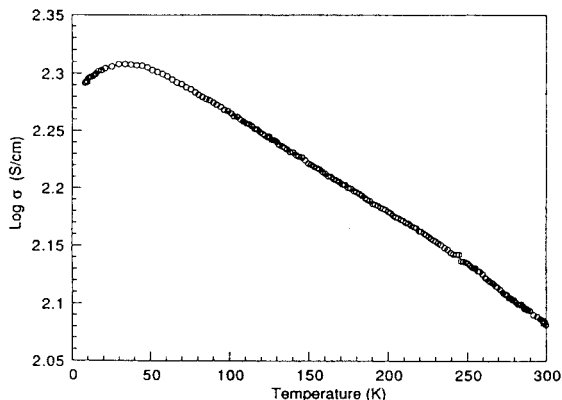
(A)
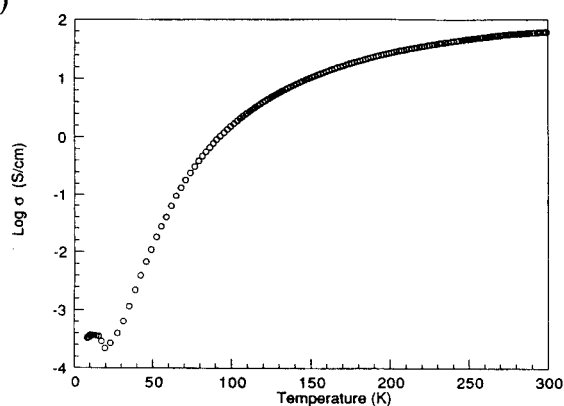
(B)

Figure 10. Variable-temperature electrical conductivity data for polycrystalline chunks of (a) $KBi_{6.33}S_{10}$ and (b) $K_2Bi_8S_{13}$.

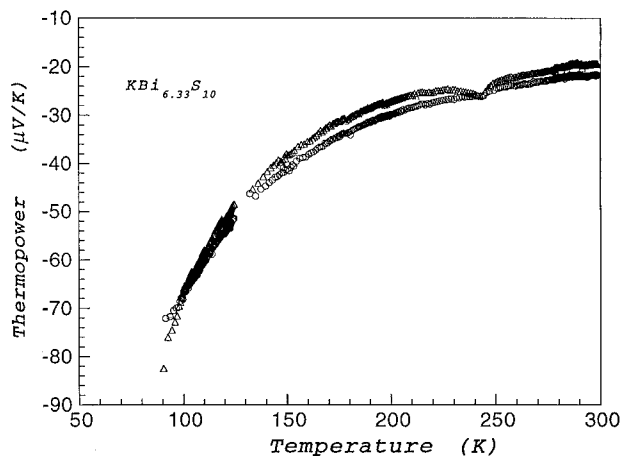**Figure 11.** Variable-temperature thermoelectric power data for polycrystalline rod of $KBi_{6.33}S_{10}$.

surements as a function of temperature. TP measurements are typically far less susceptible to artifacts arising from resistive domain boundaries in the material because they are essentially zero-current measurements. This is because temperature drops across such boundaries are much less significant than voltage drops. The TP $KBi_{6.33}S_{10}$ is negative throughout the temperature range studied ($80 < T < 300$ K) with values of $\sim -30 \ \mu$V/K at room temperature. This indicates electron (as opposed to hole) charge transport. The TP of becomes slightly more negative as the temperature is decreased from 300 to 80 K, (see Figure 11). This behavior in combination with the high electrical conductivity is characteristic of a degenerate semiconduc-
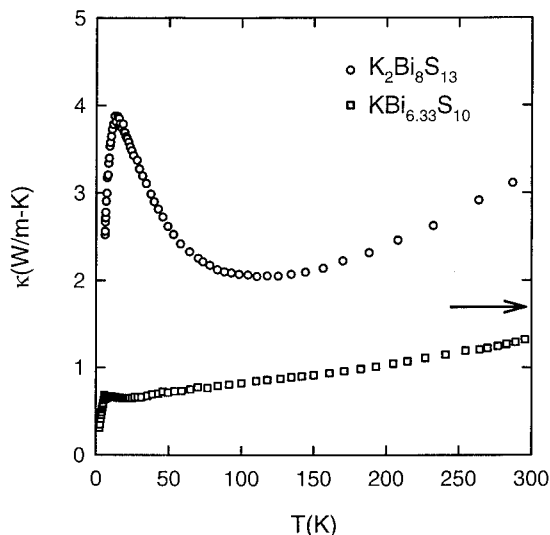

Figure 12. Temperature dependence of the thermal conductivity of polycrystalline cylindrical samples of $KBi_{6.33}S_{10}$ (open squares) and $K_2Bi_8S_{13}$ (open circles). The arrow indicates the room-temperature value of the lattice thermal conductivity of Bi_2Te_3.

tor. The semiconducting character of this material is in accord the fact that an optical gap exists in this material in the infrared region (see Figure 1a). The TP of $K_2Bi_8S_{13}$ is also negative throughout the temperature range studied ($80 < T < 300$ K) with similar magnitudes of TP at room temperature suggestive of an n-doped material. The material displays weak temperature dependence of the TP is consistent with a degenerate semiconductor. The optical gap of $K_2Bi_8S_{13}$ (Figure 1b) is quite small (<0.25 eV) similar to that of Bi_2Te_3 ($E_g = 0.16$ eV).[37] Interestingly, the TP of this material varied greatly in samples of different preparations. Seebeck coefficients as small as $-2 \ \mu$V/K were observed in some samples indicative of a heavily doped material. This discrepancy could be a result of possible nonstoichiometry ($K_{2+3x}Bi_{8-x}S_{13}$), caused by the site occupancy disorder between K and Bi found in the high coordinate Bi(8) site. The K/Bi distribution could vary from sample to sample slightly, thus affecting the electronic band structure of the Bi/S framework. Nonstoichiometry and the presence of impurities can have dramatic effects on the physical properties such as electrical conductivity and optical reflectance measurements.[38] To check if this hypothesis is true we plan substitution attempts at the Bi(8) site with other trivalent ions of similar size to Bi such as La and Ce.[39]

Thermal Conductivity. For prospective materials to be competitive for thermoelectric applications, they must possess very low thermal conductivity at the temperature range of interest. Therefore, the thermal transport properties of these materials were measured over a wide temperature region. Thermal conductivity of the two compounds is shown in Figure 12. The data show a characteristic peak at low temperatures (near 7 K for $KBi_{6.33}S_{10}$ and at around 13 K for $K_2Bi_8S_{13}$) and

(37) Li, C. Y.; Ruoff, A. L.; Spencer, C. W. *J. Appl. Phys.* **1961**, *32*, 1733.

(38) For example, SnTe is p-type with an E_g of 0.5 eV. There is uncertainty as to whether SnTe is a semiconductor or a semimetal. The high carrier concentration favors the semimetallic character of the material; however, thermoelectric power measurements suggest a semiconductor.

underscore an overall low value of thermal conductivity in these materials. $K_2Bi_8S_{13}$ shows a more pronounced peak than the one seen on the $KBi_{6.33}S_{10}$ sample and, depending on the temperature, its thermal conductivity is a factor of 2−4 larger. Using the measured values of the electrical resistivity in conjunction with the Wiedemann−Franz law, we estimate the maximum possible value of the electronic thermal conductivity contribution to be below 1% of the total thermal conductivity for $K_2Bi_8S_{13}$ and not to exceed 1−2% in the case of $KBi_{6.33}S_{10}$. Thus, essentially all heat in these compounds is carried by lattice phonons. Taking as a bench mark the room temperature value of the lattice thermal conductivity of Bi_2Te_3 ($\kappa_L \sim 1.7$ W/m K), we note that the total thermal conductivity of $KBi_{6.33}S_{10}$ is actually lower than this number. Hence, at least from the perspective of thermal transport, these compounds satisfy one of the key requirements for a useful thermoelectric material, they possess very low lattice thermal conductivity. This is an important finding because the $KBi_{6.33}S_{10}$ is a sulfide and, compared to the heavier tellurides, is expected to possess higher thermal conductvity. This is because of the higher frequency lattice phonons present in the sulfide. The surprisingly low thermal conductivity of $KBi_{6.33}S_{10}$ suggests other factors such as actual structure and lattice size and symmetry play an important role. If ways could be found to enhance the electrical conductivity and, at the same time, preserve or even increase the thermopower, at least in the case of $KBi_{6.33}S_{10}$, one indeed might have a promising thermoelectric material. To achieve this we need additional information regarding the transport properties including carrier concentrations and mobilities. Then optimization of these properties could be accomplished by controlling accurately the stoichiometry of these materials. This work is currently underway.[39]

Concluding Remarks

In summary, our investigations of the K_2S/Bi_2S_3 system have revealed two new phases, $KBi_{6.33}S_{10}$ and $K_2Bi_8S_{13}$ with new structure types. These compounds are n-type semiconductors with optical bandgaps < 0.25 eV and very good room-temperature conductivity. Although the thermoelectric power is too low for practical applications as thermoelectric materials, the product of electrical conductivity and thermopower are promising enough to warrant more systematic explorations in the A_2Q/Bi_2Q_3 (A = K, Rb, Cs; Q = S, Se, Te) and related systems.[40]

It is noteworthy that both compounds possess rather low thermal conductivity with that of $KBi_{6.33}S_{10}$ being extraordinarily low and much lower than that of Bi_2Te_3. This has the important implication that, as a class of materials, the sulfides are excellent candidates for exploration as potential thermoelectrics. The advantage of the sulfides relative to the tellurides, of course, lies in the significantly lower cost and weight savings that could be realized during manufacturing.

Supporting Information Available: Tables of atomic coordinates of all atoms and anisotropic and isotropic thermal parameters of all non-hydrogen atoms, bond distances and angles (22 pages); a listing of calculated and observed ($10F_o/10F_c$) structure factors (21 pages). Ordering information is given on any current masthead page.

CM9600182

(39) Chung, D. Y.; Iordanidis, L.; Kanatzidis, M. G., work in progress.